

Search for New Physics in Photon-Lepton Events in $p\bar{p}$ Collisions at $\sqrt{s} = 1.8$ TeV

D. Acosta,¹³ T. Affolder,²⁴ H. Akimoto,⁴⁷ M. G. Albrow,¹² D. Ambrose,³⁴ D. Amidei,²⁶ K. Anikeev,²⁵ J. Antos,¹ G. Apollinari,¹² T. Arisawa,⁴⁷ A. Artikov,¹⁰ T. Asakawa,⁴⁵ W. Ashmanskas,⁹ F. Azfar,³² P. Azzi-Bacchetta,³³ N. Bacchetta,³³ H. Bachacou,²⁴ W. Badgett,¹² S. Bailey,¹⁷ P. de Barbaro,³⁸ A. Barbaro-Galtieri,²⁴ V. E. Barnes,³⁷ B. A. Barnett,²⁰ S. Baroiant,⁵ M. Barone,¹⁴ G. Bauer,²⁵ F. Bedeschi,³⁵ S. Belforte,⁴⁴ W. H. Bell,¹⁶ G. Bellettini,³⁵ J. Bellinger,⁴⁸ D. Benjamin,¹¹ J. Bensinger,⁴ A. Beretvas,¹² J. P. Berge,¹² J. Berryhill,⁹ A. Bhatti,³⁹ M. Binkley,¹² M. Bishai,¹² D. Bisello,³³ R. E. Blair,² C. Blocker,⁴ K. Bloom,²⁶ B. Blumenfeld,²⁰ S. R. Blusk,³⁸ A. Bocci,³⁹ A. Bodek,³⁸ G. Bolla,³⁷ Y. Bonushkin,⁶ D. Bortoletto,³⁷ J. Boudreau,³⁶ A. Brandl,²⁸ S. van den Brink,²⁰ C. Bromberg,²⁷ M. Brozovic,¹¹ E. Brubaker,²⁴ N. Bruner,²⁸ J. Budagov,¹⁰ H. S. Budd,³⁸ K. Burkett,¹⁷ G. Busetto,³³ A. Byon-Wagner,¹² K. L. Byrum,² S. Cabrera,¹¹ P. Calafura,²⁴ M. Campbell,²⁶ W. Carithers,²⁴ D. Carlsmith,⁴⁸ J. Carlson,²⁶ W. Caskey,⁵ A. Castro,³ D. Cauz,⁴⁴ A. Cerri,³⁵ A. W. Chan,¹ P. S. Chang,¹ P. T. Chang,¹ J. Chapman,²⁶ C. Chen,³⁴ Y. C. Chen,¹ M. -T. Cheng,¹ M. Chertok,⁵ G. Chiarelli,³⁵ I. Chirikov-Zorin,¹⁰ G. Chlachidze,¹⁰ F. Chlebana,¹² L. Christofek,¹⁹ M. L. Chu,¹ J. Y. Chung,³⁰ W. -H. Chung,⁴⁸ Y. S. Chung,³⁸ C. I. Ciobanu,³⁰ A. G. Clark,¹⁵ A. P. Colijn,¹² A. Connolly,²⁴ M. Convery,³⁹ J. Conway,⁴⁰ M. Cordelli,¹⁴ J. Cranshaw,⁴² R. Culbertson,¹² D. Dagenhart,⁴⁶ S. D'Auria,¹⁶ S. Dell'Agnello,¹⁴ M. Dell'Orso,³⁵ L. Demortier,³⁹ M. Deninno,³ F. DeJongh,¹² S. Demers,³⁸ P. F. Derwent,¹² T. Devlin,⁴⁰ J. R. Dittmann,¹² A. Dominguez,²⁴ S. Donati,³⁵ J. Done,⁴¹ M. D'Onofrio,³⁵ T. Dorigo,¹⁷ I. Dunietz,¹² N. Eddy,¹⁹ K. Einsweiler,²⁴ J. E. Elias,¹² E. Engels, Jr.,³⁶ R. Erbacher,¹² D. Errede,¹⁹ S. Errede,¹⁹ Q. Fan,³⁸ H.-C. Fang,²⁴ R. G. Feild,⁴⁹ J. P. Fernandez,¹² C. Ferretti,³⁵ R. D. Field,¹³ I. Fiori,³ B. Flaughner,¹² G. W. Foster,¹² M. Franklin,¹⁷ J. Freeman,¹² J. Friedman,²⁵ H. J. Frisch,⁹ Y. Fukui,²³ I. Furic,²⁵ S. Galeotti,³⁵ A. Gallas,²⁹ M. Gallinaro,³⁹ T. Gao,³⁴ M. Garcia-Sciveres,²⁴ A. F. Garfinkel,³⁷ P. Gatti,³³ C. Gay,⁴⁹ D. W. Gerdes,²⁶ E. Gerstein,⁸ P. Giannetti,³⁵ K. Giolo,³⁷ V. Glagolev,¹⁰ D. Glenzinski,¹² M. Gold,²⁸ J. Goldstein,¹² I. Gorelov,²⁸ A. T. Goshaw,¹¹ Y. Gotra,³⁶ K. Goulianos,³⁹ C. Green,³⁷ G. Grim,⁵ P. Gris,¹² C. Grosso-Pilcher,⁹ M. Guenther,³⁷ G. Guillian,²⁶ J. Guimaraes da Costa,¹⁷ R. M. Haas,¹³ C. Haber,²⁴ S. R. Hahn,¹² C. Hall,¹⁷ T. Handa,¹⁸ R. Handler,⁴⁸ F. Happacher,¹⁴ K. Hara,⁴⁵ A. D. Hardman,³⁷ R. M. Harris,¹² F. Hartmann,²¹ K. Hatakeyama,³⁹ J. Hauser,⁶ J. Heinrich,³⁴ A. Heiss,²¹ M. Herndon,²⁰ C. Hill,⁵ A. Hocker,³⁸ K. D. Hoffman,⁹ R. Hollebeek,³⁴ L. Holloway,¹⁹ B. T. Huffman,³² R. Hughes,³⁰ J. Huston,²⁷ J. Huth,¹⁷ H. Ikeda,⁴⁵ J. Incandela,¹² G. Introzzi,³⁵ A. Ivanov,³⁸ J. Iwai,⁴⁷ Y. Iwata,¹⁸ E. James,²⁶ M. Jones,³⁴ U. Joshi,¹² H. Kambara,¹⁵ T. Kamon,⁴¹ T. Kaneko,⁴⁵ M. Karagoz Unel,²⁹ K. Karr,⁴⁶ S. Kartal,¹² H. Kasha,⁴⁹ Y. Kato,³¹ T. A. Keaffaber,³⁷ K. Kelley,²⁵ M. Kelly,²⁶ R. D. Kennedy,¹² D. Khazins,¹¹ T. Kikuchi,⁴⁵ B. Kilminster,³⁸ B. J. Kim,²² D. H. Kim,²² H. S. Kim,¹⁹ M. J. Kim,⁸ S. B. Kim,²² S. H. Kim,⁴⁵ Y. K. Kim,²⁴ M. Kirby,¹¹ M. Kirk,⁴ L. Kirsch,⁴ S. Klimenko,¹³ P. Koehn,³⁰ K. Kondo,⁴⁷ J. Konigsberg,¹³ A. Korn,²⁵ A. Korytov,¹³ E. Kovacs,² J. Kroll,³⁴ M. Kruse,¹¹ V. Krutelyov,⁴¹ S. E. Kuhlmann,² K. Kurino,¹⁸ T. Kuwabara,⁴⁵ A. T. Laasanen,³⁷ N. Lai,⁹ S. Lami,³⁹ S. Lammel,¹² J. Lancaster,¹¹ M. Lancaster,²⁴ R. Lander,⁵ A. Lath,⁴⁰ G. Latino,²⁸ T. LeCompte,² K. Lee,⁴² S. W. Lee,⁴¹ S. Leone,³⁵ J. D. Lewis,¹² M. Lindgren,⁶ T. M. Liss,¹⁹ D. O. Litvintsev,¹² J. B. Liu,³⁸ T. Liu,¹² Y. C. Liu,¹ O. Lobban,⁴² N. S. Lockyer,³⁴ J. Loken,³² M. Loreti,³³ D. Lucchesi,³³ P. Lukens,¹² S. Lusin,⁴⁸ L. Lyons,³² J. Lys,²⁴ P. McIntyre,⁴¹ R. Madrak,¹⁷ K. Maeshima,¹² P. Maksimovic,¹⁷ L. Malferrari,³ G. Manca,³² M. Mangano,³⁵ M. Mariotti,³³ G. Martignon,³³ A. Martin,⁴⁹ V. Martin,²⁹ J. A. J. Matthews,²⁸ P. Mazzanti,³ K. S. McFarland,³⁸ M. Menguzzato,³³ A. Menzione,³⁵ P. Merkel,¹² C. Mesropian,³⁹ A. Meyer,¹² T. Miao,¹² J. S. Miller,²⁶ R. Miller,²⁷ H. Minato,⁴⁵ S. Miscetti,¹⁴ M. Mishina,²³ G. Mitselmakher,¹³ Y. Miyazaki,³¹ N. Moggi,³ E. Moore,²⁸ R. Moore,²⁶ Y. Morita,²³ T. Moulik,³⁷ A. Mukherjee,¹² M. Mulhearn,²⁵ T. Muller,²¹ A. Munar,³⁵ P. Murat,¹² S. Murgia,²⁷ J. Nachtman,⁶ V. Nagaslaev,⁴² S. Nahn,⁴⁹ H. Nakada,⁴⁵ I. Nakano,¹⁸ C. Nelson,¹² T. Nelson,¹² C. Neu,³⁰ D. Neuberger,²¹ C. Newman-Holmes,¹² C.-Y. P. Ngan,²⁵ H. Niu,⁴ L. Nodulman,² A. Nomerotski,¹³ S. H. Oh,¹¹ Y. D. Oh,²² T. Ohmoto,¹⁸ T. Ohsugi,¹⁸ R. Oishi,⁴⁵ T. Okusawa,³¹ J. Olsen,⁴⁸ W. Orejudos,²⁴ C. Pagliarone,³⁵ F. Palmonari,³⁵ R. Paoletti,³⁵ V. Papadimitriou,⁴² D. Partos,⁴ J. Patrick,¹² G. Pauletta,⁴⁴ C. Paus,²⁵ M. Paulini,⁸ D. Pellett,⁵ L. Pescara,³³ T. J. Phillips,¹¹ G. Piacentino,³⁵ K. T. Pitts,¹⁹ A. Pompos,³⁷ G. Pope,³⁶ T. Pratt,³² F. Prokoshin,¹⁰ J. Proudfoot,² F. Ptohos,¹⁴ O. Pukhov,¹⁰ G. Punzi,³⁵ A. Rakitine,²⁵ F. Ratnikov,⁴⁰ D. Reher,²⁴ A. Reichold,³² P. Renton,³² A. Ribon,³³ W. Riegler,¹⁷ F. Rimondi,³ L. Ristori,³⁵ M. Riveline,⁴³ W. J. Robertson,¹¹ T. Rodrigo,⁷ S. Rolli,⁴⁶ L. Rosenson,²⁵ R. Roser,¹² R. Rossin,³³ C. Rott,³⁷ A. Roy,³⁷ A. Ruiz,⁷ A. Safonov,⁵ R. St. Denis,¹⁶ W. K. Sakumoto,³⁸ D. Saltzberg,⁶ C. Sanchez,³⁰ A. Sansoni,¹⁴ L. Santi,⁴⁴ H. Sato,⁴⁵ P. Savard,⁴³ A. Savoy-Navarro,¹² P. Schlabach,¹² E. E. Schmidt,¹² M. P. Schmidt,⁴⁹ M. Schmitt,²⁹ L. Scodellaro,³³ A. Scott,⁶ A. Scribano,³⁵ A. Sedov,³⁷ S. Segler,¹²

S. Seidel,²⁸ Y. Seiya,⁴⁵ A. Semenov,¹⁰ F. Semeria,³ T. Shah,²⁵ M. D. Shapiro,²⁴ P. F. Shepard,³⁶ T. Shibayama,⁴⁵ M. Shimojima,⁴⁵ M. Shochet,⁹ A. Sidoti,³³ J. Siegrist,²⁴ A. Sill,⁴² P. Sinervo,⁴³ P. Singh,¹⁹ A. J. Slaughter,⁴⁹ K. Sliwa,⁴⁶ C. Smith,²⁰ F. D. Snider,¹² A. Solodsky,³⁹ J. Spalding,¹² T. Speer,¹⁵ M. Spezziga,⁴² P. Sphicas,²⁵ L. Spiegel,¹² F. Spinella,³⁵ M. Spiropulu,⁹ J. Steele,⁴⁸ A. Stefanini,³⁵ J. Strogas,¹⁹ F. Strumia,¹⁵ D. Stuart,¹² K. Sumorok,²⁵ T. Suzuki,⁴⁵ T. Takano,³¹ R. Takashima,¹⁸ K. Takikawa,⁴⁵ P. Tamburello,¹¹ M. Tanaka,⁴⁵ B. Tannenbaum,⁶ M. Tecchio,²⁶ P. K. Teng,¹ K. Terashi,³⁹ R. J. Tesarek,¹² S. Tether,²⁵ A. S. Thompson,¹⁶ E. Thomson,³⁰ R. Thurman-Keup,² P. Tipton,³⁸ S. Tkaczyk,¹² D. Toback,⁴¹ K. Tollefson,³⁸ A. Tollestrup,¹² D. Tonelli,³⁵ M. Tonnesmann,²⁷ H. Toyoda,³¹ W. Trischuk,⁴³ J. F. de Troconiz,¹⁷ J. Tseng,²⁵ D. Tsybychev,¹³ N. Turini,³⁵ F. Ukegawa,⁴⁵ T. Vaiculis,³⁸ J. Valls,⁴⁰ E. Vataga,³⁵ S. Vejcik III,¹² G. Velev,¹² G. Veramendi,²⁴ R. Vidal,¹² I. Vila,⁷ R. Vilar,⁷ I. Volobouev,²⁴ M. von der Mey,⁶ D. Vucinic,²⁵ R. G. Wagner,² R. L. Wagner,¹² W. Wagner,²¹ N. B. Wallace,⁴⁰ Z. Wan,⁴⁰ C. Wang,¹¹ M. J. Wang,¹ S. M. Wang,¹³ B. Ward,¹⁶ S. Waschke,¹⁶ T. Watanabe,⁴⁵ D. Waters,³² T. Watts,⁴⁰ R. Webb,⁴¹ M. Webber,²⁴ H. Wenzel,²¹ W. C. Wester III,¹² A. B. Wicklund,² E. Wicklund,¹² T. Wilkes,⁵ H. H. Williams,³⁴ P. Wilson,¹² B. L. Winer,³⁰ D. Winn,²⁶ S. Wolbers,¹² D. Wolinski,²⁶ J. Wolinski,²⁷ S. Wolinski,²⁶ S. Worm,⁴⁰ X. Wu,¹⁵ J. Wyss,³⁵ U. K. Yang,⁹ W. Yao,²⁴ G. P. Yeh,¹² P. Yeh,¹ J. Yoh,¹² C. Yosef,²⁷ T. Yoshida,³¹ I. Yu,²² S. Yu,³⁴ Z. Yu,⁴⁹ J. C. Yun,¹² A. Zanetti,⁴⁴ and F. Zetti²⁴

¹*Institute of Physics, Academia Sinica, Taipei, Taiwan 11529, Republic of China*

²*Argonne National Laboratory, Argonne, Illinois 60439*

³*Istituto Nazionale di Fisica Nucleare, University of Bologna, I-40127 Bologna, Italy*

⁴*Brandeis University, Waltham, Massachusetts 02254*

⁵*University of California at Davis, Davis, California 95616*

⁶*University of California at Los Angeles, Los Angeles, California 90024*

⁷*Instituto de Fisica de Cantabria, CSIC-University of Cantabria, 39005 Santander, Spain*

⁸*Carnegie Mellon University, Pittsburgh, PA 15218*

⁹*Enrico Fermi Institute, University of Chicago, Chicago, Illinois 60637*

¹⁰*Joint Institute for Nuclear Research, RU-141980 Dubna, Russia*

¹¹*Duke University, Durham, North Carolina 27708*

¹²*Fermi National Accelerator Laboratory, Batavia, Illinois 60510*

¹³*University of Florida, Gainesville, Florida 32611*

¹⁴*Laboratori Nazionali di Frascati, Istituto Nazionale di Fisica Nucleare, I-00044 Frascati, Italy*

¹⁵*University of Geneva, CH-1211 Geneva 4, Switzerland*

¹⁶*Glasgow University, Glasgow G12 8QQ, United Kingdom*

¹⁷*Harvard University, Cambridge, Massachusetts 02138*

¹⁸*Hiroshima University, Higashi-Hiroshima 724, Japan*

¹⁹*University of Illinois, Urbana, Illinois 61801*

²⁰*The Johns Hopkins University, Baltimore, Maryland 21218*

²¹*Institut für Experimentelle Kernphysik, Universität Karlsruhe, 76128 Karlsruhe, Germany*

²²*Center for High Energy Physics: Kyungpook National University, Taegu 702-701; Seoul National University, Seoul 151-742; and SungKyunKwan University, Suwon 440-746; Korea*

²³*High Energy Accelerator Research Organization (KEK), Tsukuba, Ibaraki 305, Japan*

²⁴*Ernest Orlando Lawrence Berkeley National Laboratory, Berkeley, California 94720*

²⁵*Massachusetts Institute of Technology, Cambridge, Massachusetts 02139*

²⁶*University of Michigan, Ann Arbor, Michigan 48109*

²⁷*Michigan State University, East Lansing, Michigan 48824*

²⁸*University of New Mexico, Albuquerque, New Mexico 87131*

²⁹*Northwestern University, Evanston, Illinois 60208*

³⁰*The Ohio State University, Columbus, Ohio 43210*

³¹*Osaka City University, Osaka 588, Japan*

³²*University of Oxford, Oxford OX1 3RH, United Kingdom*

³³*Universita di Padova, Istituto Nazionale di Fisica Nucleare, Sezione di Padova, I-35131 Padova, Italy*

³⁴*University of Pennsylvania, Philadelphia, Pennsylvania 19104*

³⁵*Istituto Nazionale di Fisica Nucleare, University and Scuola Normale Superiore of Pisa, I-56100 Pisa, Italy*

³⁶*University of Pittsburgh, Pittsburgh, Pennsylvania 15260*

³⁷*Purdue University, West Lafayette, Indiana 47907*

³⁸*University of Rochester, Rochester, New York 14627*

³⁹*Rockefeller University, New York, New York 10021*

⁴⁰*Rutgers University, Piscataway, New Jersey 08855*

⁴¹*Texas A&M University, College Station, Texas 77843*

⁴²*Texas Tech University, Lubbock, Texas 79409*

⁴³*Institute of Particle Physics, University of Toronto, Toronto M5S 1A7, Canada*

⁴⁴*Istituto Nazionale di Fisica Nucleare, University of Trieste/Udine, Italy*

⁴⁵University of Tsukuba, Tsukuba, Ibaraki 305, Japan

⁴⁶Tufts University, Medford, Massachusetts 02155

⁴⁷Waseda University, Tokyo 169, Japan

⁴⁸University of Wisconsin, Madison, Wisconsin 53706

⁴⁹Yale University, New Haven, Connecticut 06520

(Dated: March 17, 2002)

We present the results of a search in $p\bar{p}$ collisions at $\sqrt{s} = 1.8$ TeV for anomalous production of events containing a photon and a lepton (e or μ), both with large transverse energy, using 86 pb^{-1} of data collected with the Collider Detector at Fermilab during the 1994-95 collider run at the Fermilab Tevatron. The presence of large missing transverse energy (\cancel{E}_T), additional photons, or additional leptons in these events is also analyzed. The results are consistent with standard model expectations, with the possible exception of photon-lepton events with large \cancel{E}_T , for which the observed total is 16 events and the expected mean total is 7.6 ± 0.7 events.

PACS numbers: 13.85.Rm, 12.60.Jv, 13.85.Qk, 14.80.Ly

An important test of the standard model (SM) of particle physics [1] is to measure and understand the properties of the highest-energy particle collisions. The observation of an anomalous production rate of any combination of the fundamental fermions and bosons of the SM would be a clear indication of a new physical process. This Letter summarizes an analysis of the inclusive production of a photon and a lepton (e or $\mu + \gamma + X$), including searches for the associated production of additional photons, leptons, and large missing transverse energy, using 86 pb^{-1} of data from proton-antiproton collisions collected with the Collider Detector at Fermilab (CDF) during the 1994-95 run of the Fermilab Tevatron [2].

Production of these particular combinations of particles is of interest for several reasons. Events with photons and leptons are potentially related to the puzzling “ $ee\gamma\cancel{E}_T$ ” event recorded by CDF [3]. A supersymmetric model [4] designed to explain the $ee\gamma\cancel{E}_T$ event predicts the production of photons from the radiative decay of the $\tilde{\chi}_2^0$ neutralino, and leptons through the decay of charginos, indicating $\ell\gamma\cancel{E}_T$ events as a signal for the production of a chargino-neutralino pair. Other hypothetical, massive particles could subsequently decay to SM electroweak gauge bosons, one of which could be a photon and the other a W or Z^0 boson that decays leptonically. In addition, photon-lepton studies complement similarly-motivated inclusive searches for new physics in diphoton [5], photon-jet [6], and photon- b -quark events [7].

The CDF detector [8] is a cylindrically symmetric spectrometer designed to study $p\bar{p}$ collisions at the Fermilab Tevatron. A superconducting solenoid of length 4.8 m and radius 1.5 m generates a magnetic field of 1.4 T and contains tracking chambers used to measure the momenta of charged particles. A set of vertex time projection chambers is used to find the z position [9] of the $p\bar{p}$ interaction. The 3.5-m-long central tracking chamber (CTC) is a wire drift chamber which provides up to 84 measurements between the radii of 31.0 cm and 132.5 cm in the region $|\eta| < 1.0$. Sampling calorimeters, used to measure the electromagnetic and hadronic energy

deposited by electrons, photons, and jets of hadrons, surround the solenoid. The calorimeter is segmented into towers that project to $z = 0$ and consist of an electromagnetic section followed by a hadronic section. Each tower of the central ($|\eta| < 1.1$) electromagnetic calorimeter (CEM) has embedded in it a strip chamber that allows the measurement of the 2-dimensional transverse profile of electromagnetic showers. Muons are detected with three systems of muon chambers, each consisting of four layers of drift chambers. The central muon (CMU) system is located directly outside the central hadronic calorimeter, and covers $|\eta| < 0.6$. Outside of the CMU is 0.6 m of steel shielding, followed by the central muon upgrade system. The central muon extension system provides muon detection for $0.6 < |\eta| < 1.0$.

Events with a high-transverse momentum (p_T) [10] photon or lepton are selected by a three-level trigger [2], which requires an event to have either a high- E_T photon or a high- p_T lepton (e or μ) within the central region, $|\eta| < 1.0$. Photon and electron candidates are chosen from clusters of energy in adjacent CEM towers; electrons are then further separated from photons by requiring the presence of a CTC track pointing at the cluster. Muons are identified by requiring CTC tracks to extrapolate to a reconstructed track segment in the muon drift chambers.

To reduce background from the production of photons or leptons from the decays of hadrons produced in jets, both the photon and the lepton in each event are required to be ‘isolated’. The transverse energy deposited in the calorimeters in a cone in $\eta - \phi$ space of radius $R = 0.4$ around the photon or lepton position is summed, and the E_T due to the photon or lepton is subtracted. The remaining energy in the cone, E_{cone}^{iso} , is required to be less than 2 GeV for a photon, or less than 10% of the lepton transverse momentum. In addition, for photons the sum of the momenta of all CTC tracks in the cone must be less than 5 GeV.

Inclusive photon-lepton events are selected by requiring an isolated central photon with $E_T^\gamma > 25$ GeV and an isolated central lepton (e or μ) with $E_T^\ell > 25$ GeV. The

technical criteria used to identify leptons and photons are very similar to those of Refs. [5–7], and are described in detail in Ref. [2]. A total of 77 events pass this selection: 29 photon-muon and 48 photon-electron candidates.

The production of pairs of new heavy states that decay via cascade decays can lead to final states with multiple photons or leptons; in contrast, the dominant SM background processes lead to signatures with only one photon and one lepton observed in the detector, as discussed in detail below. The inclusive sample is consequently analyzed as two subsamples: a “two-body inclusive photon-lepton sample” typical of a two-particle final state, and a “multi-body inclusive photon-lepton sample” typical of three or more particles in the final state. The two-body sample selection requires exactly one photon and exactly one lepton, with an azimuthal separation $\Delta\varphi_{\ell\gamma} > 150^\circ$, but excludes those events for which the invariant mass of the photon and electron, $M_{e\gamma}$, is within 5 GeV of M_Z (these events are used as a control sample, as described below). The multi-body sample is composed of the remaining inclusive photon-lepton events. The multi-body sample is then further analyzed for the presence of large \cancel{E}_T , and additional leptons and photons. The \cancel{E}_T threshold of 25 GeV was determined *a priori* in previous analyses [13] as a significant indicator of a neutrino arising from leptonic decays of the W boson. Figure 1 shows the breakdown of the inclusive sample into the final categories.

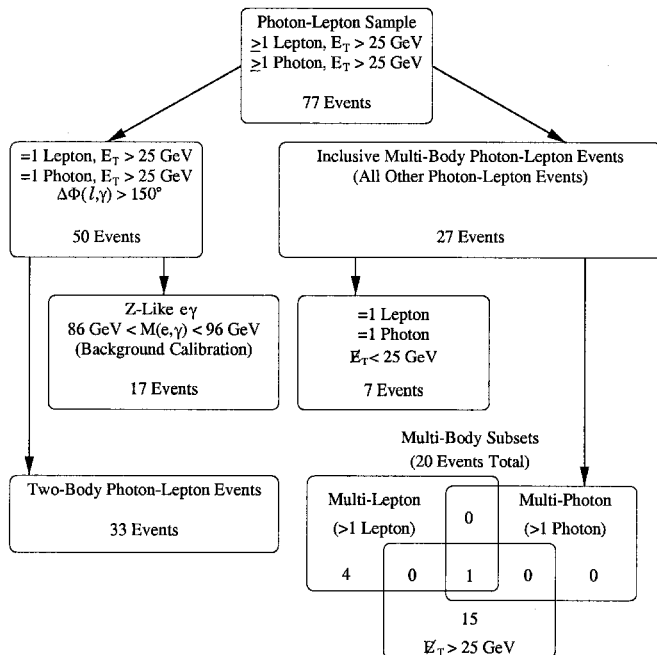


FIG. 1: The subsets of inclusive photon-lepton events. The multi-body photon-lepton subcategories of $\ell\gamma\cancel{E}_T$, multi-lepton, and multi-photon events are not mutually exclusive.

The dominant source of photon-lepton events at the Tevatron is electroweak diboson production, in which a W or Z^0 boson decays leptonically ($\ell\nu$ or $\ell\ell$) and a photon is radiated from either an initial-state quark, a W , or a charged final-state lepton. The number of such events is estimated using leading-order (LO) matrix element calculations [15] for which the computational code [16] was then embedded into the general-purpose event generator program PYTHIA [17], followed by a full simulation of the detector. The uncertainty in this number has roughly equal contributions from higher order processes (the K-factor), simulation systematics, luminosity, proton structure, and generator statistics.

A jet of hadrons initiated by a quark or gluon can contain mesons such as the π^0 or η that decay to photons, which then may satisfy the photon selection criteria. The number of lepton-plus-misidentified-jet events is determined by counting the number of jets in lepton data and then multiplying by the probability of a jet being misidentified as a photon, P_γ^{jet} . The factor P_γ^{jet} is determined from samples of jets and photons in events with a lepton trigger, using the distribution in E_{cone}^{iso} . By fitting the data to a sum of the distribution for prompt photons, measured from identified electrons, and that for jets, the misidentification rate is found to be $P_\gamma^{jet} = (3.8 \pm 0.7) \times 10^{-4}$, as shown in Figure 2.

The dominant source of misidentified photon-electron events is $Z^0 \rightarrow e^+e^-$ production, where one of the electrons undergoes hard photon bremsstrahlung or a track fails to be reconstructed. We assume that photon-electron events consistent with Z^0 production are not a significant source of new physics, and use them to estimate the probability P_γ^e that an electron is reconstructed as a photon. The number of misidentified photon-electron events in the control sample divided by the number of electron-electron pairs with the same kinematics gives $P_\gamma^e = (1.28 \pm 0.35)\%$. For any other subset of central electron pairs, the contribution to the corresponding photon-electron sample is the product of P_γ^e and the number of central electron pairs.

Other, smaller, backgrounds are due to hadrons faking muons, and to leptons from the decay of bottom and charm quarks. A hadron jet generally contains charged hadrons, which may penetrate the calorimeters into the muon chambers, or which may decay to a muon before reaching the calorimeters. These contributions are determined by identifying isolated, high-momentum tracks in the photon data, determining the probability of each track being misidentified as a muon, and summing this probability over all tracks in the sample [2]. The contribution to photon-lepton candidates from heavy-flavor produced in association with a prompt photon is estimated using Monte Carlo event generation [17] and detector simulation, and found to be negligible.

New physics in small samples of events would most likely manifest itself as an excess of observed events over

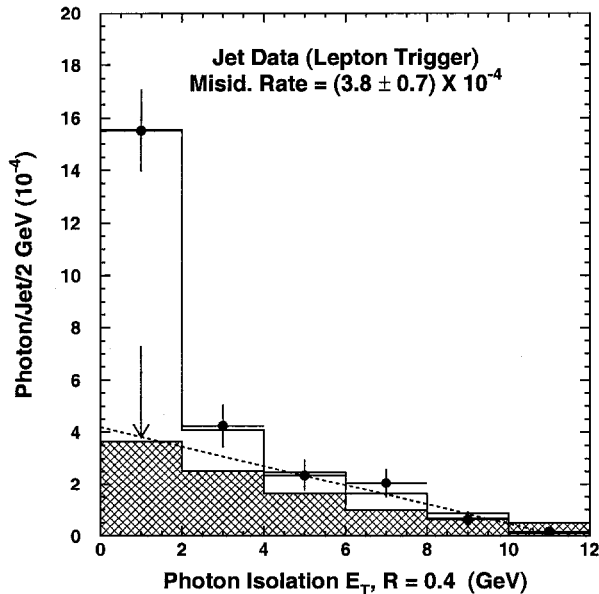


FIG. 2: The number of photon candidates per jet as a function of E_{cone}^{iso} , for jet data obtained with a lepton trigger. Included are data (points), the fit (solid line), the jet component of the fit (dotted line), and a Monte Carlo estimate of the contribution from W plus jet events using the PYTHIA event generator with the CDF detector simulation (cross-hatched histogram). The arrow indicates the value of E_{cone}^{iso} at which the misidentification rate P_{γ}^{jet} is determined.

expected events. In the absence of a specific alternative model, the significance of an observed excess is computed from the likelihood of obtaining at least the observed number of events, N_0 , assuming that the null hypothesis (the SM) is correct. The “observation likelihood”, $P(N \geq N_0 | \mu_{SM})$, is defined as the fraction of the Poisson distribution for the number of expected events from SM sources, with a mean μ_{SM} , that yields outcomes $N \geq N_0$ [18]. The likelihood $P(N \geq N_0 | \mu_{SM})$ is computed from a large ensemble of calculations in which each quantity used to compute photon-lepton event sources varies randomly as a Gaussian distribution, and the resulting mean event total is used to randomly generate a Poisson-distributed outcome N . The fraction of calculations in the ensemble with outcomes $N \geq N_0$ gives $P(N \geq N_0 | \mu_{SM})$.

The predicted and observed totals for two-body photon-lepton events are compared in Table I. Half of the predicted total originates from $Z^0\gamma$ production where one of the charged leptons has escaped identification; the other half originates from roughly equal contributions of $W\gamma$ production, misidentified jets, misidentified electrons, and misidentified charged hadrons. The likelihood of the observed event total is 9.3%.

Process	Two-Body		Multi-Body	
	$\ell\gamma X$	$\ell\gamma X$	$\ell\gamma\cancel{E}_T X$	$\ell\ell\gamma X$
$W+\gamma$	2.7 ± 0.3	5.0 ± 0.6	3.9 ± 0.5	–
$Z+\gamma$	12.5 ± 1.2	9.6 ± 0.9	1.3 ± 0.2	5.5 ± 0.6
$\ell+\text{jet}, \text{jet} \rightarrow \gamma$	3.3 ± 0.7	3.2 ± 0.6	2.1 ± 0.4	0.3 ± 0.1
$Z \rightarrow ee, e \rightarrow \gamma$	4.1 ± 1.1	1.7 ± 0.5	0.1 ± 0.1	–
Hadron $+\gamma$	1.4 ± 0.7	0.5 ± 0.3	0.2 ± 0.1	–
π/K Decay $+\gamma$	0.8 ± 0.9	0.3 ± 0.3	0.1 ± 0.1	–
b/c Decay $+\gamma$	0.1 ± 0.1	< 0.01	< 0.01	–
Predicted μ_{SM}	24.9 ± 2.4	20.2 ± 1.7	7.6 ± 0.7	5.8 ± 0.6
Observed N_0	33	27	16	5
$P(N \geq N_0 \mu_{SM})$	9.3%	10.0%	0.7%	68.0%

TABLE I: The mean numbers μ_{SM} of two-body and inclusive multi-body events predicted by the SM, the number N_0 observed, and the observation likelihood $P(N \geq N_0 | \mu_{SM})$. Correlated uncertainties have been taken into account.

The predicted and observed totals for inclusive multi-body photon-lepton events are also compared in Table I. About half of the predicted total originates from $Z^0\gamma$ production, a quarter from $W\gamma$ production, and the remaining quarter from particles misidentified as photons or leptons. The likelihood of the observed inclusive multi-body total is 10%. The predicted and observed kinematic distributions for these events are compared in Figure 3. The difference between the observed and predicted totals can be entirely attributed to events with $\cancel{E}_T > 25$ GeV. Figure 3 also shows the distribution in H_T , the scalar sum of the E_T of all objects in the event plus the magnitude of \cancel{E}_T , a variable correlated with the production of massive particles [2].

The predicted and observed totals for multi-body $\ell\gamma\cancel{E}_T$ events are also compared in Table I. For photon-electron events, requiring $\cancel{E}_T > 25$ GeV suppresses the contributions from $Z^0\gamma$ production and from electrons misidentified as photons, which have no intrinsic \cancel{E}_T , while preserving the contribution from $W\gamma$ production. As a result, 57% of the predicted $e\gamma\cancel{E}_T$ total arises from $W\gamma$ production, 31% from jets misidentified as photons, only 3% from $Z^0\gamma$ production, and the remaining 9% from other particles misidentified as photons. The observed $e\gamma\cancel{E}_T$ total agrees with the predicted total, with a 25% probability that the predicted mean total of 3.4 events yields 5 observed events. One of these 5 is the $ee\gamma\cancel{E}_T$ event [3].

For photon-muon events, requiring $\cancel{E}_T > 25$ GeV does not completely eliminate the contribution from $Z^0\gamma$, for if the second muon has $|\eta| > 1.2$ and $p_T > 25$ GeV it escapes detection and induces the necessary amount of \cancel{E}_T . The rate at which this occurs is modeled well by the $Z^0\gamma$ event simulation, however, since it is largely a function of the CDF detector geometric acceptance. Of the 4.6 multi-body events predicted to originate from $Z^0\gamma$ production, 2.2 events are predicted to contain a second visible muon, 1.0 events are predicted to have

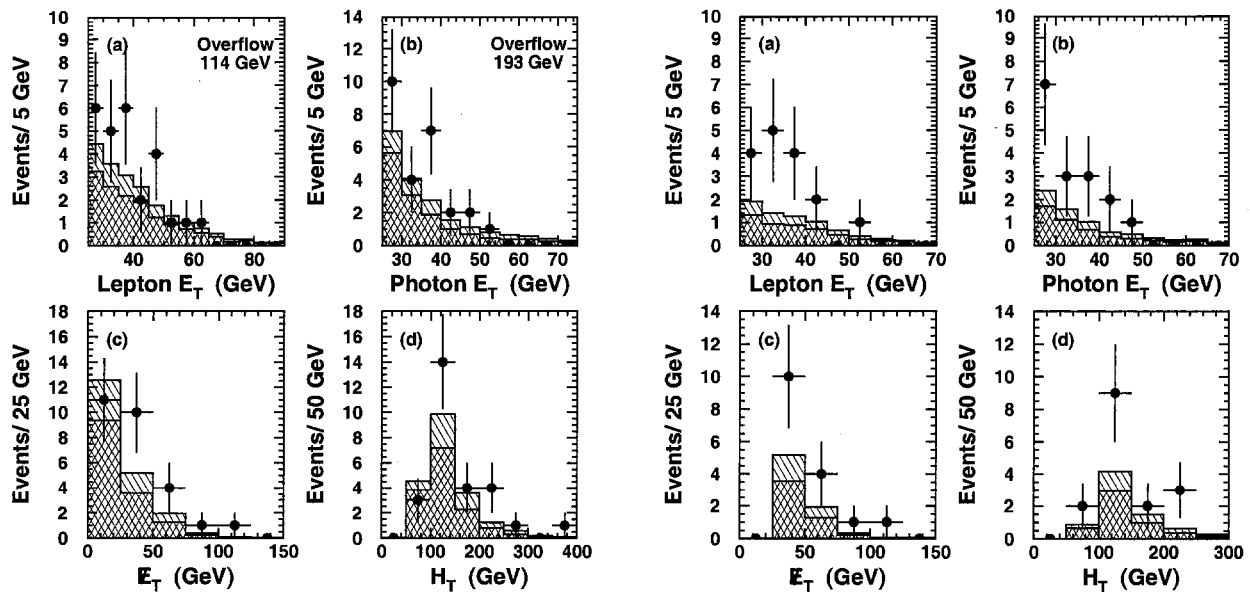


FIG. 3: Left: The lepton E_T , photon E_T , \cancel{E}_T , and H_T of inclusive multi-body photon-lepton candidates (points) compared to SM predictions (single-hatched histograms). The cross-hatched histograms show the contribution from SM $W\gamma$ and $Z\gamma$ production. There is one event in the overflow bin at 114 GeV in a) and one at 193 GeV in b). Right: The same distributions for the subset of these events that have $\cancel{E}_T > 25$ GeV.

less than 25 GeV of \cancel{E}_T , and only 1.0 events are predicted to pass the 25 GeV \cancel{E}_T selection. One event is observed with a second visible muon, in agreement with the $Z^0\gamma$ prediction. The predicted total for multi-body $\mu\gamma\cancel{E}_T$ events consists of 47% $W\gamma$ production, 24% events with jets misidentified as photons, 23% $Z^0\gamma$ production, and the remaining 7% from other particles misidentified as muons.

The observed $\mu\gamma\cancel{E}_T$ event total is higher than predicted (11 observed vs. 4 expected), with an observation likelihood of 0.54%; the observation likelihood of the $\ell\gamma\cancel{E}_T$ total is only slightly higher at 0.72% [19]. The predicted and observed distributions of the kinematic properties of multi-body $\ell\gamma\cancel{E}_T$ events are compared in Figure 3. The observed photon E_T , lepton E_T , \cancel{E}_T , and H_T distributions are within the range expected from the standard model.

The predicted and observed totals of multi-lepton events are compared in Table I. Nearly all of the predicted total is expected from $Z^0\gamma$ production. Approximately 6 events are expected; 5 events are observed, including the $ee\gamma\gamma\cancel{E}_T$ event. No $e\mu\gamma$ events were expected, and none were observed.

The predicted number of multi-photon events is dominated by $Z\gamma$ production, for which only 0.01 events are expected. The single event observed is the $ee\gamma\gamma\cancel{E}_T$ event, whose (un)likelihood is described in Ref. [3].

In conclusion, we have made an *a priori* search for in-

clusive photon+lepton production. We find that subsamples of this data set agree well with their SM prediction, with the possible exception of $\gamma\ell\cancel{E}_T$. However, an excess of events with 0.7% likelihood (equivalent to 2.7 standard deviations for a Gaussian distribution) in one subsample among the five studied is an interesting result, but it is not a compelling observation of new physics. We look forward to more data in the upcoming run of the Fermilab Tevatron.

We thank the Fermilab staff and the technical staffs of the participating institutions for their contributions. We thank U. Baur and S. Mrenna for their critical calculations of the SM $W\gamma$ and $Z\gamma$ backgrounds used in this analysis. This work was supported by the U.S. Department of Energy and National Science Foundation; the Italian Istituto Nazionale di Fisica Nucleare; the Ministry of Education, Culture, Sports, Science, and Technology of Japan; the Natural Sciences and Engineering Research Council of Canada; the National Science Council of the Republic of China; the Swiss National Science Foundation; the A. P. Sloan Foundation; the Bundesministerium fuer Bildung und Forschung, Germany; the Korea Science and Engineering Foundation (KoSEF); the Korea Research Foundation; and the Comision Interministerial de Ciencia y Tecnologia, Spain.

-
- [1] S. L. Glashow, Nucl. Phys. **22** 588, (1961); S. Weinberg, Phys. Rev. Lett. **19** 1264, (1967); A. Salam, Proc. 8th Nobel Symposium, Stockholm, (1979).
- [2] A longer description of this analysis is available in D. Acosta *et al.*, submitted to Phys. Rev. D (hep-ex/0110015).
- [3] F. Abe *et al.*, Phys. Rev. D **59**, 092002 (1999).
- [4] See, for example, S. Ambrosanio, G. L. Kane, G. D. Kribs, S. P. Martin, and S. Mrenna, Phys. Rev. D **55**, 1372 (1997); for a recent (post Ref. 2) interpretation see: B.C. Allanach, S. Lola, K. Sridhar, CERN-TH-2001-360.
- [5] T. Affolder *et al.*, Phys. Rev. D **64**, 092002 (2001); F. Abe *et al.*, Phys. Rev. Lett **81**, 1791 (1998). See also: P. Achard *et al.*, Phys. Lett. **B527** 29, (2002); G. Abbiendi *et al.*, Eur. Phys. J. C **18** 253, (2000); P. Abreu *et al.*, Eur. Phys. J. C **17** 53, (2000); R. Barate *et al.*, Eur. Phys. J. C **16** 71, (2000); B. Abbott *et al.*, Phys. Rev. Lett. **82**, 2244 (1999); B. Abbott *et al.*, Phys. Rev. Lett. **81**, 524 (1998); B. Abbott *et al.*, Phys. Rev. Lett. **80**, 442 (1998); S. Abachi *et al.*, Phys. Rev. Lett. **78**, 2070 (1997).
- [6] B. Abbott *et al.*, Phys. Rev. Lett. **82**, 29 (1999).
- [7] F. Abe *et al.*, Phys. Rev. Lett **83**, 3124 (1999).
- [8] A detailed description can be found in F. Abe *et al.*, Nucl. Instrum. Methods Phys. Res., Sect. A **271**, 387 (1988).
- [9] The CDF coordinate system of r , φ , and z is cylindrical, with the z -axis along the proton beam. The pseudorapidity is $\eta = -\ln(\tan(\theta/2))$.
- [10] The transverse momentum is defined as $p_T = p \sin \theta$; the transverse energy is defined as $E_T = E \sin \theta$. Missing transverse energy is defined as $\cancel{E}_T = -\Sigma E_T$, where the sum is over all objects in an event. We use the convention that ‘momentum’ refers to pc and ‘mass’ to mc^2 , so that energy, momentum, and mass are all measured in GeV.
- [11] T. Affolder *et al.*, Phys. Rev. D **63**, 032003 (2001); F. Abe *et al.*, Phys. Rev. D **50**, 2966 (1994).
- [12] J. Berryhill, Ph.D. thesis, University of Chicago, 2000.
- [13] F. Abe *et al.*, Phys. Rev. D **52**, 2624 (1995).
- [14] F. Abe *et al.*, Phys. Rev. D **45**, 1448 (1992).
- [15] U. Baur and E. L. Berger, Phys. Rev. D **47**, 4889 (1993); **41**, 1476 (1990).
- [16] U. Baur and S. Mrenna, private communication. The source code is available publicly at <http://moose.ucdavis.edu/mrenna/code>.
- [17] T. Sjostrand, Computer Physics Commun. **82** (1994) 74; S. Mrenna, Computer Physics Commun. **101** (1997) 232.
- [18] The uncertainty in μ_{SM} is the standard deviation of a large ensemble of calculations, and takes into account correlated uncertainties.
- [19] It is important to note that any muon-electron difference is statistically insignificant; the probability that 16 events divide up into two categories as asymmetrically as 11 to 5 or higher is greater than 8%.